JPE 7-1-1

# Synthesis and Experimental Implementation of DSP Based Backstepping Control of Positioning Systems

Jie Chang†, and Yaolong Tan*

†*Electrical and Computer Engineering, Florida State University

**ABSTRACT**

Novel nonlinear backstepping control with integrated adaptive control function is developed for high-performance positioning control systems. The proposed schemes are synthesized by a systematic approach and implemented based on a modern low-cost DSP controller, TMS320C32. A baseline backstepping control scheme is derived first, and is then extended to include a nonlinear adaptive control against the system parameter changes and load variations. The backstepping control utilizes Lyapunov function to guarantee the convergence of the position tracking error. The final control algorithm is a convenient in the implementation of a practical 32-bit DSP controller. The new control system can achieve superior performance over the conventional nested PI controllers, with improved position tracking, control bandwidth, and robustness against external disturbances, which is demonstrated by experimental results.

**Keywords:** back-stepping control approach, synthesis of multi-loop system, position tracking, DSP-based digital control systems

## 1. Introduction

The common control method for today's industrial motion control products is based on a classical linear system design approach using nested PI controllers in a multiple-feedback-loop structure. In this structure, a PI or PID controller is employed in the positioning and inner velocity control loop, respectively. Such a control method provides acceptable performance in many motion control applications where the performance requirement is not high. However, when the system parameter changes become significant, i.e. large inertia variations and large sudden load disturbances, it is difficult to achieve a fast response and satisfactory robustness. On the other hand, the cross-interaction between the outer and inner feedback control loops could not be conveniently incorporated by the traditional nested PI-control loop approach, thus limiting the performance of the system

In recent years, significant efforts of developing nonlinear control approaches have been made for industrial applications[1-6]. However, the majority of the previous works did not present a step-by-step design methodology and did not incorporate practical control implementation using a modern DSP or microprocessor.

In this paper, a baseline backstepping control scheme incorporating an integral function is systematically derived first in Section 2 after formulating the motion control problem for convenient analysis and synthesis. It is

Manuscript received July. 24, 2006; revised Sep. 4, 2006.
† Corresponding Author: jchang@caps.fsu.edu, Florida State Univ.
Tel: +850-410-6562, Fax: +850-410-6368
*Electrical and Computer Engineering, Florida State University

then extended in Section 3 to include a nonlinear adaptive control scheme against the system's parameter and load variations. The objectives are to improve the system's bandwidth and robustness against the parameter variations and load disturbances under a constraint of limited bandwidth of the inner torque-control loop. In addition, a practical DSP based digital control system is implemented and discussed. The experimental implementation and effectiveness of the proposed control scheme are demonstrated and verified by experimental results in Section 5 and 6. The experimental results show that the new control scheme can obtain superior performance over the conventional method of motion control.

## 2. Problem Formulation and Synthesis of Backstepping Control with an Integral Function

A simplified second-order model of a mechanical motion system is given below:

$$\frac{d\theta}{dt} = \omega,$$
$$J\frac{d\omega}{dt} = T_q - T_L \tag{1}$$

where $\theta$ is the angular position, $\omega$ is the angular velocity, $J$ is the total effective mechanical inertia on the motor shaft. $T_q$ is the electromagnetic torque generated by the AC motor and $T_L$ is the load torque on the rotating shaft. The key system variables are defined and listed in Nomenclature. In this paper, $T_q$ is the control input to the motion system in (1). It can be assumed at this stage that the inertia $J$ is a known positive constant that can be calibrated at a rated operating point. Our goal is to design a new control scheme to achieve close and asymptotical tracking for a given bounded position reference signal $\theta_{ref}$, while keeping the system's state trajectory within a bounded range that is governed by the practical physical limitations. By assumption, the given reference signal $\theta_{ref}$ is a continuous and differentiable signal. This assumption does not impose any difficulties in a practical application. In fact, a front-processing stage providing a shaped input reference signal via a digital low-pass filter is often used in today's industrial motion control applications.

While the conventional control design starts from the most inner feedback loop and moves out stage by stage, backstepping control approach works on the most outer loop first and moves in an inward direction. The synthesis includes four main stages: (1) Position control stage. (2) Angular velocity control stage. (3) Proof of asymptotic tracking. (4) Parameter estimation and adaptive control. A list of key symbols is also provided at the end of this paper.

### 2.1 Synthesis Stage 1: Positioning Control

First, define the position tracking error $e1$ and its derivative:

$$e_1 = \theta_{ref} - \theta$$
$$\frac{de_1}{dt} = \dot{\theta}_{ref} - \omega \tag{2}$$

The definition above is directly related to the control objective: to minimize the position tracking error.

Since the angular velocity $\omega$ should be the control reference input to the next control stage, we simply choose $\omega$ to render the exponential convergence for the system's state trajectory. A first-order differential equation is obtained and given by:

$$\omega = c_1 e_1 + \dot{\theta}_{ref}, \tag{3}$$

where $c_1$ is a positive constant. Considering equation (2), this leads to a desired exponential converging behavior for the tracking error $e_1$:

$$\frac{de_1}{dt} = -c_1 e_1. \tag{4}$$

Since the angular velocity $\omega$ will be a control reference variable, we assign $\omega$ as a "virtual" control in reference to the next control stage that is the angular

velocity control of the AC motor. In a practical system, an integral control term can be added to equation. (3) and a new differential equation for the "virtual" control $\omega$ is obtained and given by:

$$\omega_{ref} = c_1 e_1 + \dot{\theta}_{ref} + \lambda_1 \chi_1 \tag{5}$$

where $\lambda_1$ is a positive constant and $\chi_1 = \int_0^t e_1(\tau)d\tau$ is the integral of the position tracking error. By integrating the integral action into the "virtual" control function [1], the tracking error e1 can be forced down and converged to zero at the steady-state despite the external disturbances and parameter inaccuracy of the system modeling. For convenient reference, a flowchart of our systematic synthesis of this backstepping control system is presented in Figure 1 and the major design stages will be detailed in the following sections.

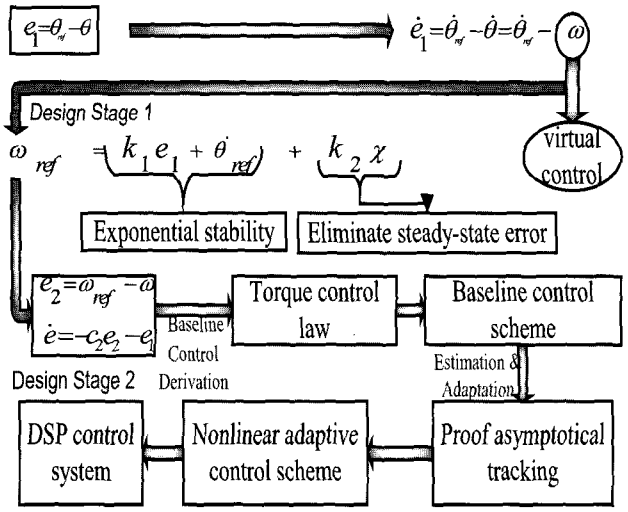


Fig. 1 Flowchart of systematic synthesis of backstepping control approach

### 2.2 Synthesis Stage 2: Angular Velocity Control

The velocity tracking error and its derivative can be described by the differential equation in (6):

$$e_2 = \omega_{ref} - \omega$$
$$\frac{de_2}{dt} = c_1(\dot{\theta}_{ref} - \omega) + \ddot{\theta}_{ref} + \lambda_1 e_1 - \frac{T_q}{J}, \tag{6}$$

where $e_2 = \omega_{ref} - \omega$ shows the velocity tracking error. The desirable transient function of the position tracking in (2) can then be rewritten related to e2:

$$\frac{de_1}{dt} = -c_1 e_1 - \lambda_1 \chi_1 + e_2. \tag{7}$$

For convenient synthesis and control implementation, equation (6) can be rewritten to explicitly relate to the state variables and error signals, such as $e_1$, $e_2$, and the integral position tracking error $\chi_1$ that are physically measurable:

$$\frac{de_2}{dt} = c_1 \frac{de_1}{dt} + \ddot{\theta}_{ref} + \lambda_1 e_1 - \frac{T_q}{J}$$
$$= c_1(-c_1 e_1 - \lambda_1 \chi_1 + e_2) + \ddot{\theta}_{ref} + \lambda_1 e_1 - \frac{T_q}{J}. \tag{8}$$

Wherein equation (8) uses the expression of $\dot{e}_1$ defined by equation (7).

As shown in equation (6) and (8), the torque command, $T_q$, acts as a control input to the electromechanical system. A differential equation in (9) can be selected such that it will lead to an exponential rate of asymptotic convergence of e2 and a desirable torque control law:

$$\frac{de_2}{dt} = -c_2 e_2 - e_1 \tag{9}$$

Substituting eqn. (9) to (8), a torque control law for the AC servo is derived and given as:

$$T_q = J\{(1 - c_1^2 + \lambda_1)e_1 + (c_1 + c_2)e_2 - c_1\lambda_1\chi_1 + \ddot{\theta}_{ref}\} \tag{10}$$

where $c_2$ is a positive constant and it actually determines the convergence speed of the velocity tracking loop.

### 2.3 Analysis of New Control Scheme and Asymptotical Tracking

We have so far completed an algorithm development of

a backstepping positioning control system as given by eqn (1)-(6) and (10). In order to facilitate a convenient analysis and control implementation, it is beneficial and desirable to convert the algorithm in differential equations into a new control scheme that can be understood by industrial control engineers. Figure 2 shows a control block diagram of the proposed new backstepping control scheme that clearly highlights the system's control architecture and control signal flow.

By an observation of Figure 2, it is interesting to find that a new feedforward control path is created; as highlighted a dashed block with a transfer function of $1+C_1^2+\lambda_1$, which is not available in a conventional control scheme. This new control function takes the position error signal, e1, and directly feeds it to the control summation point for the torque producing command of the AC servo with a predetermined amplification gain. The feedforward control function bypasses two regulators at the positioning feedback control stage and the velocity feedback control stage, respectively, where large mechanical time constant or slow transient responses exist, thus reducing the control time delay. This inter-loop bridging control is therefore desirable for improving the system's control bandwidth, response speed and robustness against external disturbances. The backstepping control scheme also employs an integral control function at its positioning regulation stage to eliminate the tracking error in the steady state.

On the other hand, the new backstepping control scheme preserves all desirable substructures of the conventional motion control systems, including feedforward velocity and acceleration signals of the position reference input, $\dot{\theta}_{ref}$ and $\ddot{\theta}_{ref}$. However, the new control scheme does not require any additional tuning for these feedforward gains as required by the conventional approach. This is because the gains are already normalized as a unity at this stage and have naturally become an integrated part of the new control scheme.

It should also be mentioned that presently a well-designed torque-producing current loop commonly has a high bandwidth, i.e. over 1000 Hz. In comparison, the bandwidth of the positioning control loop is often below 10 Hz. The bandwidth difference makes it possible to simplify the transfer function of the power amplifier that has inner current control loop(s)[7]. Therefore in Figure 2, the torque producing current loop is assumed as an ideal amplifier having a unity gain for its transfer function without affecting the genuineness of the control synthesis when performing an analysis or design of the outer control loops. The synthesis, which begins from the outer to inner control stages, also makes it convenient to adapt this model reduction.

The system's stability and asymptotic convergence can be further verified based on the Lyapunov function approach. We choose the following Lyapunov energy

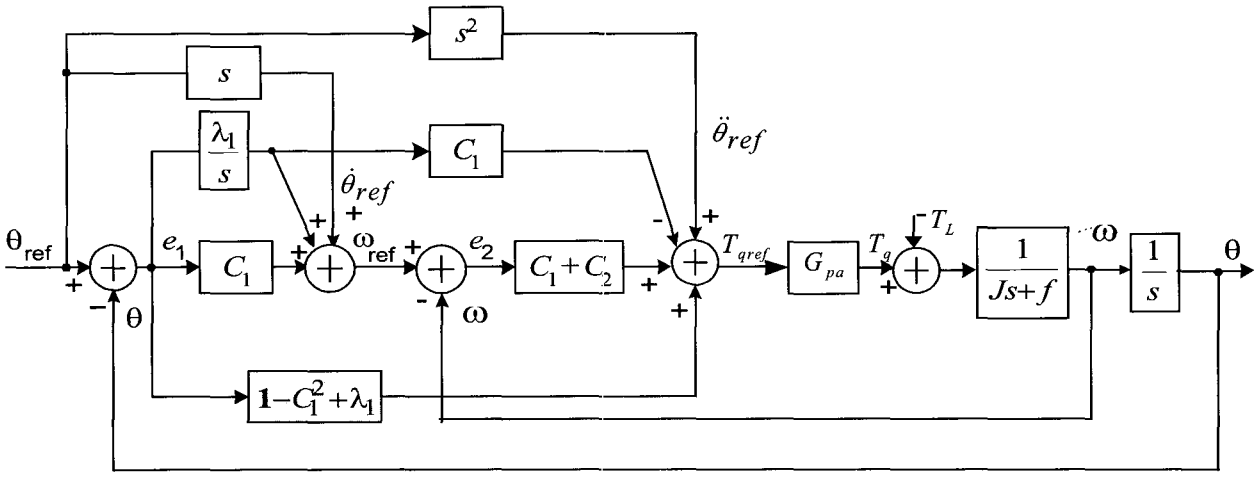


Fig. 2 Block diagram of backstepping control scheme with integration function

function for the closed-loop control system:

$$V=\frac{\lambda_1}{2}\chi_1^2+\frac{1}{2}e_1^2+\frac{1}{2}e_2^2, \tag{11}$$

where the position tracking error $e_1$ and its integration $\chi_1$, and velocity tracking error $e_2$ are included.

Considering the desirable system state trajectories given in (7) for the positioning control and (9) for velocity control, the derivative of the Lyapunov function can be obtained as:

$$\dot{V}=-c_1e_1^2-c_2e_2^2\le 0 \tag{12}$$

A proof of the system's asymptotic convergence is given in Appendix A.

## 3. Estimation and Adaptive Control for Inertia Changes and Load Disturbances

The synthesis of backstepping control in Section 2 can be extended to integrate the estimation of the system's mechanical inertia and sudden load changes, and control adaptation into the process.

At the design stage 2, consider the load disturbance TL and redefine equation (8) as:

$$\frac{de_2}{dt}=c_1(\dot{\theta}_{ref}-\omega)+\ddot{\theta}_{ref}+\lambda_1e_1-\frac{T_q}{J}+\frac{T_L}{J} \tag{13}$$

where TL is the load disturbance torque. The task is to estimate the inertia variations and the load disturbance using an algorithm that can be integrated with the backstepping control. We assume J and TL are positive constants and can be determined for a particular system at a rated operating point. For convenient analysis, we define a new variable representing the ratio of TL and J:

$$\Gamma=\frac{T_L}{J}. \tag{14}$$

The strategy is then to estimate the effect of the load disturbance on the velocity tracking dynamics in (13), instead of estimating the load disturbance, TL, directly. Therefore (13) can be rewritten as:

$$\frac{de_2}{dt}=c_1(\dot{\theta}_{ref}-\omega)+\ddot{\theta}_{ref}+\lambda_1e_1-\frac{T_q}{J}+\Gamma \tag{15}$$

The effective inertia, J, and normalized load disturbance, Γ, now become adaptation parameters of the control system. From equation (7) and (15), equation (16) can be obtained:

$$\begin{aligned}\frac{de_2}{dt}&=c_1\frac{de_1}{dt}+\ddot{\theta}_{ref}+\lambda_1e_1-\frac{T_q}{J}+\Gamma\\&=c_1\left(-c_1e_1-\lambda_1\chi_1+e_2\right)+\ddot{\theta}_{ref}+\lambda_1e_1-\frac{T_q}{J}+\Gamma,\end{aligned} \tag{16}$$

Since the actual values of the effective inertia, J, and normalized load disturbance, Γ, change in real time, we replace them with their estimates, $\hat{J}$ and $\hat{\Gamma}$. By a similar approach taken in Section 2, a desirable torque control law can be obtained and given in eqn. (17):

$$T_q=\hat{J}\left\{(1-c_1^2+\lambda_1)e_1+(c_1+c_2)e_2-c_1\lambda_1\chi_1+\ddot{\theta}_{ref}+\hat{\Gamma}\right\} \tag{17}$$

The next step is to derive the update laws for the parameter estimates, $\hat{J}$ and $\hat{\Gamma}$. For this purpose, we define the parameter estimation error signals as:

$$\tilde{J}=J-\hat{J},\quad \tilde{\Gamma}=\Gamma-\hat{\Gamma} \tag{18}$$

Substituting the torque command in (17) back to the velocity tracking error dynamics in (16) obtains:

$$\begin{aligned}\frac{de_2}{dt}=&-c_2e_2-e_1+\frac{\tilde{J}}{J}\left\{(1-c_1^2+\lambda_1)e_1+(c_1+c_2)e_2\right.\\&\left.-c_1\lambda_1\chi_1+\ddot{\theta}_{ref}+\hat{\Gamma}\right\}+\tilde{\Gamma}.\end{aligned} \tag{19}$$

A constructive Lyapunov design approach can then be used to obtain the update laws for the parameter estimates, $\hat{J}$ and $\hat{\Gamma}$. The Lyapunov energy function for the closed-loop system is chosen as:

$$V=\frac{\lambda_1}{2}\chi_1^2+\frac{1}{2}e_1^2+\frac{1}{2}e_2^2+\frac{1}{2\gamma_1J}\tilde{J}^2+\frac{1}{2\gamma_2}\tilde{\Gamma}^2, \tag{20}$$

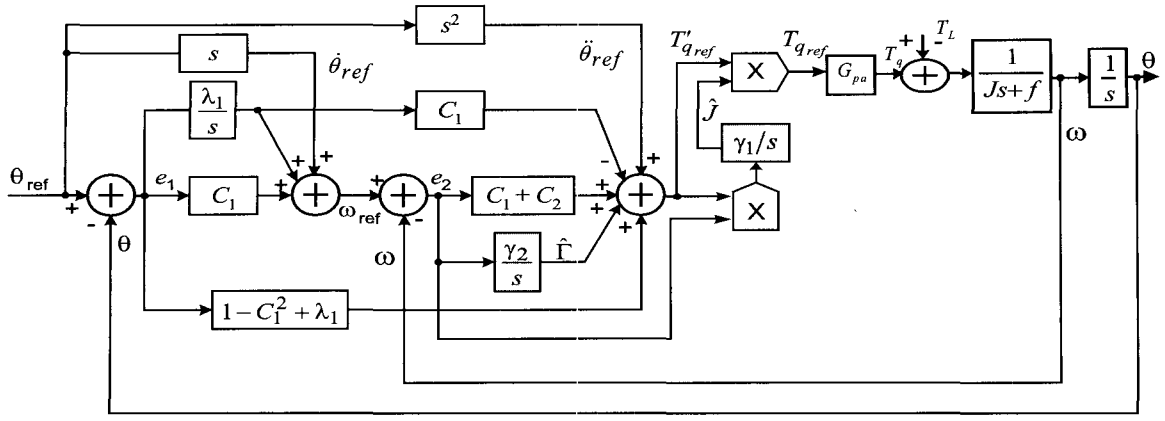


Fig. 3 New control scheme of adaptive backstepping motion control

where γ1 and γ2 are positive design constants and they determine the convergence speed of the estimation errors. Along the closed-loop tracking trajectories specified in the equations (7) and (19), a derivative of the Lyapunov function can be given in eqn. (21):

$$\begin{aligned}\dot{V} &= \lambda_1\chi_1\dot{\chi}_1 + e_1\dot{e}_1 + e_2\dot{e}_2 + \frac{\tilde{J}}{\gamma_1 J}(-\frac{d\hat{J}}{dt}) + \frac{\tilde{\Gamma}}{\gamma_2}(-\frac{d\hat{\Gamma}}{dt}) \\ &= -c_1e_1^2 - c_2e_2^2 + \frac{\tilde{J}}{J}\{e_2[(1-c_1^2+\lambda_1)e_1 + (c_1+c_2)e_2 \\ &\quad - c_1\lambda_1\chi_1 + \ddot{\theta}_{ref} + \hat{\Gamma}] - \frac{1}{\gamma_1}\frac{d\hat{J}}{dt}\} + \tilde{\Gamma}\{e_2 - \frac{1}{\gamma_2}\frac{d\hat{\Gamma}}{dt}\}.\end{aligned} \tag{21}$$

In order to render the non-positivity of the Lyapunov derivative in the above equation, we now choose the adaptation laws for the parameter estimates, $\hat{J}$ and $\hat{\Gamma}$ as:

$$\begin{aligned}\frac{d\hat{J}}{dt} &= \gamma_1 e_2\{(1-c_1^2+\lambda_1)e_1 + (c_1+c_2)e_2 - c_1\lambda_1\chi_1 + \ddot{\theta}_{ref} + \hat{\Gamma}\} \\ \frac{d\hat{\Gamma}}{dt} &= \gamma_2 e_2.\end{aligned} \tag{22}$$

Inspecting eqn. (21) and (22), it can be found that the adaptation law in (22) cancels out undesirable dynamics and allows the terms associated with $\tilde{J}$ and $\tilde{\Gamma}$ in the Lyapunov derivative in (21) to converge to zero [5]. This renders the following desirable behavior for the closed-loop system:

$$\dot{V} = -c_1e_1^2 - c_2e_2^2 \le 0. \tag{23}$$

A new control scheme of adaptive backstepping control can be obtained based on eqn (1)-(6), (17) and (22) as illustrated in Figure 3. In comparison with the first scheme of our baseline backstepping control in Figure 2, Figure 3 includes additional nonlinear control blocks and parameter estimation for $\hat{J}$ and $\hat{\Gamma}$ as highlighted in the shaded blocks.

## 4. Digital Simulation Results

As aforementioned, the conventional motion control systems employ nested PI control strategy and multiple-loop structure. In particular, a linear PI controller is employed in the position and velocity loop, respectively, to accomplish feedback controls. On the other hand, our proposed backstepping control approach and scheme are based on the Lyapunov nonlinear control approach. The new control schemes inherently have nonlinear control properties and advantages as discussed in Section 2 and 3. Comparative studies of the performances are conducted by digital simulation and presented in this section.

To keep the same base operating conditions and lead to an apple-to-apple comparison, a nested-PI position control system can be conveniently reduced, for a comparative evaluation, from the control scheme in Figure 2 by setting the feed forward term from the positioning loop to the inner loop, 1+ C12 +λ1 = 0. This keeps all other control and system's parameters unchanged. A digital simulation of the tracking response of the conventional nested PI control system is shown in Figure 4. A slope reference

input is given in our simulation. The control gains for the PI controller at the positioning stage are $k_1 = 6$ for P term, $k_2 = 2$ for I term. The P term for the velocity loop is set to be 1.5. In Figure 4, the dashed line in the top subplot is the given positioning reference signal. At $t = 5s$, the servo drive is commanded to move at 60 RPM and stop at $t = 8s$. The solid line is the position response. The corresponding position tracking error is zoomed and shown in the second subplot. There is obviously a constant tracking error of about 0.16 rad during the transition of the response.

In comparison, Figure 5 shows the position response to the slope reference input of the backstepping control system. In the simulation, the controller parameters are set as: $c_1 = 6$, $c_2 = 4$, and $\lambda_1 = 2$. The guideline of selecting the control gains in this case is to obtain an approximate critically-damped response as shown in Figure 4 and 5, which is acceptable for a good tuning for the control gains. As depicted, the average value of the tracking error has been reduced, to below 0.01 rad during the transition.

The maximum tracking error is only about 0.06 rad at the starting and ending points of the response, which is much smaller than that of the conventional nested PI controller, indicating an improvement of the performance and bandwidth.

The effect of the integral action in the backstepping control algorithm is evaluated. Figure 6 is the system response of the backstepping control system as shown in Figure 2. The integral gain is set as $\lambda_1 = 8$. At time $t = 3s$, a step load disturbance with a magnitude of -0.2 Nm is injected. A slope reference input at 1 rad/sec is then given at time $t = 5s$. The position tracking errors caused by the slope reference input and the load disturbance are small as shown in Figure 6. The bottom subplot shows the corresponding torque response.

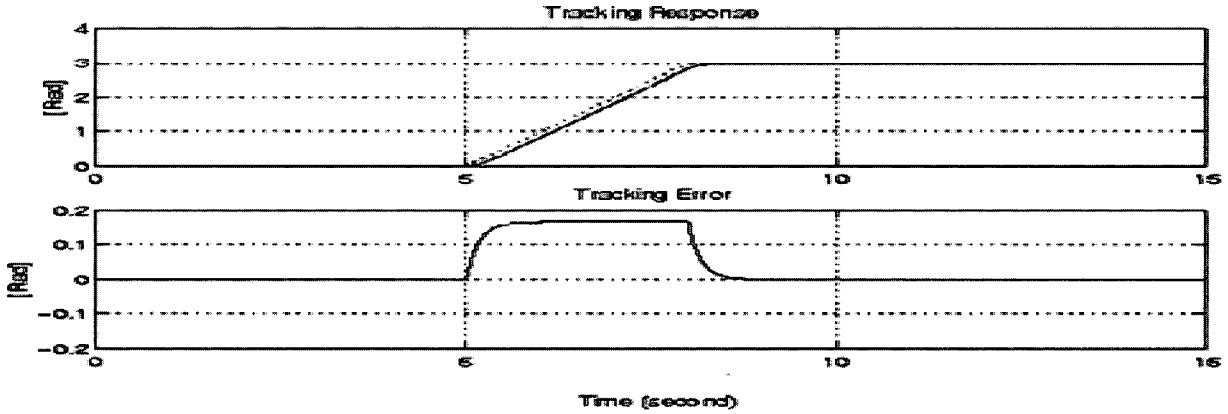


Fig. 4 Position tracking response of the conventional nested PI controller to a trapezoidal reference input.

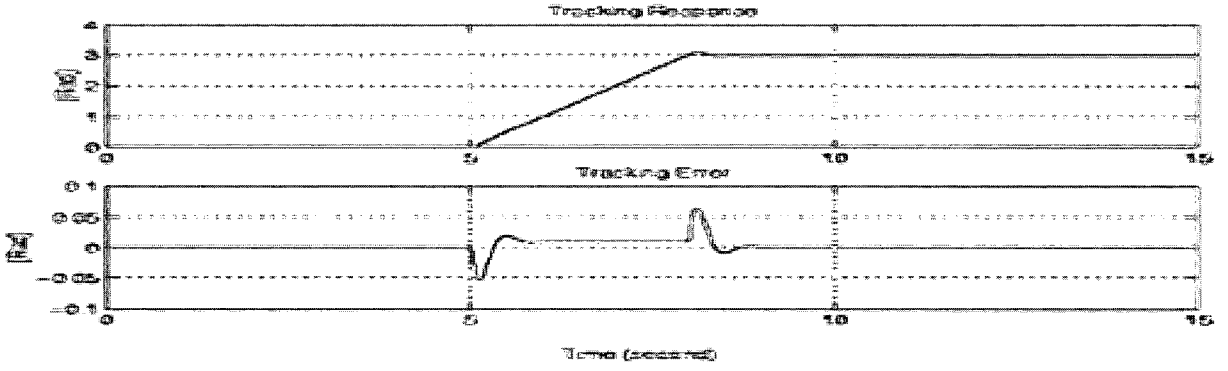

Fig. 5 Position tracking response of the backstepping nonlinear controller against a trapezoidal reference input.

In comparison, a system response of the backstepping control system with no integral function ( $\lambda_1 = 0$ ) is shown in Figure 7. The consistent steady-state tracking error can be clearly observed from the subplot 2 and subplot 3 in Figure 7. The comparison confirms the added integral action in the backstepping control can significantly reduce the steady- state tracking errors. In addition, properly increasing the integral gain of the position controller can also be beneficial to the performance for reducing the position tracking error in our system. The analysis and approach of the control gain selection for the proposed adaptive backstepping motion control is a promising subject. Preliminary research work is reported and given in our recent work [10], but can not be detailed in this paper due to the page limit.

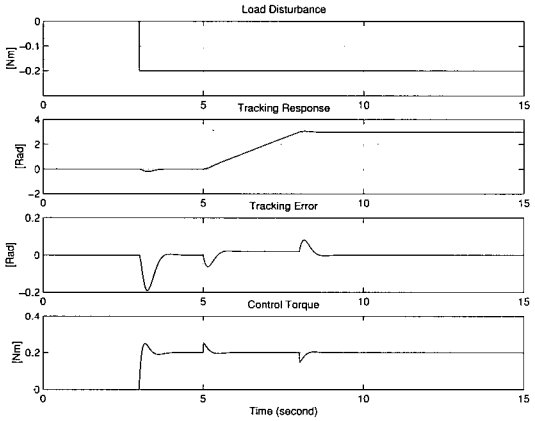


Fig. 6 Tracking response of the backstepping nonlinear controller with the integral action. Time: 50s/div.

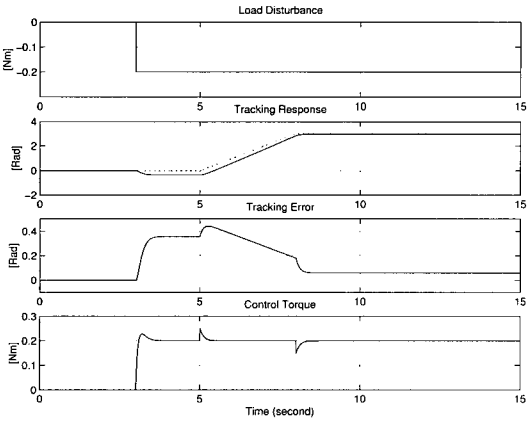


Fig. 7 Tracking response of the backstepping nonlinear controller(without the integral action) subject to a load disturbance.

## 5. System Implementation Based on a Low-Cost DSP

The motion control experiment hardware and a prototype system have been implemented based on a single-board electronic controller with a core DSP chip TMS320C32. The DSP is a low-cost 32-bit floating-point integrated controller. This chip costs less than $10 each at production volume. A hardware control system block diagram is given in Figure 8. The backstepping control schemes in Figure 2 and 3 are programmed in "C" and then debugged and loaded to the DSP for real time control.

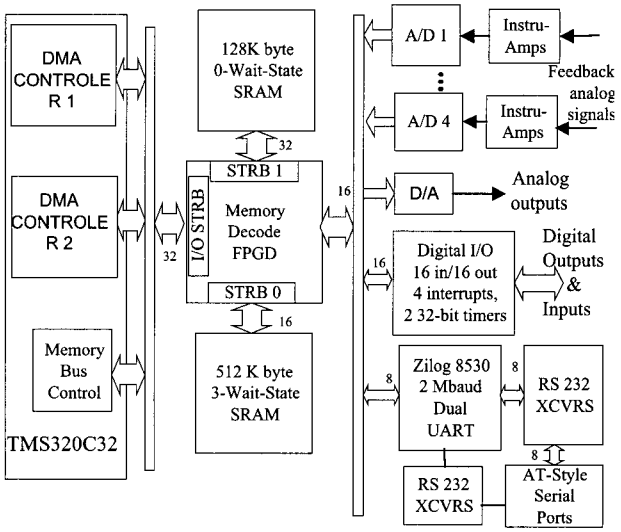


Fig. 8 Block diagram of DSP Controller based on TMS 320C32

A Lab experimental system is developed and the prototype consists of four main parts: (1) DSP controller; (2) servo power amplifier; (3) AC servo motors; and (4) Personal Computer (PC) as a graphic interface. The PC runs Texas Instruments (TI) Code Composer v3.04, which provides an integrated environment for compiling C code to the object code using TI's C compiler. The final object code is then downloaded into the DSP, TMS320C32. The PC also communicates with the DSP controller via a communication module, ControlLogix (Rockwell), that is commercially available. The DSP receives the reference control inputs from the PC and executes the algorithm of the backstepping control scheme. Encoder signals, including the position and velocity signals, provide

feedback to the DSP control module. The control output of the torque command is sent to the servo power amplifier where it employs an additional high-bandwidth digital current control [7-9]. The servo amplifiers are set to work at torque current mode, and its dynamics are much faster than the mechanical dynamics.

The Lab test servo motors are permanent magnetic AC motors, RA Y-1002-1, rated at 500W and 230VAC. The detailed motor parameters are omitted here to reduce the paper's length since the motor's time constant is insignificant in comparison with those in the position and velocity loops. In order to test the load disturbance, we programmed the second-axis servo drive to work in the torque mode and geared the two servo motors together through a belt. A voltage generator is then used to control the magnitude of the emulated load disturbance. The total moment inertia on the motor shaft is estimated to be about 0.08 kg-m$^2$. For comparison purpose, we also implemented the conventional position and velocity loop control based on the conventional nested PI control approach. In lab testing, the position reference input signal, actual position, torque command, and the motor current are monitored by the multiple-channel color digital oscilloscope, DataSYS 740, for data recording. Experimental Results

## 6. Experimental Results

Figure 9 gives an experimental result of the system output response to a slope-position input at small signal mode and the system has a traditional nested PI control. In this mode, the system's state responses will be kept within a linear range without going to saturation. Therefore, the acceleration and deceleration of the given trajectory are smaller than the maximum allowable acceleration and deceleration rates of the actual servo system. The vertical distance between $\theta$ and $\theta_{ref}$ stands for the position tracking error. As expected, during the transient dynamics, the conventional PI controller is not able to reduce the tracking error to zero since it is a "type I" linear feedback control system.

Figure 10 shows the system position response to a slope reference input of the backstepping control system. It is clear that the tracking error is substantially reduced to nearly zero with this new control scheme. The actual motor position closely tracks the slope reference input and the tacking error converges to zero rapidly. Additional observation of the control action or toque signal also shows the improvement of the system response speed. As shown in Figure 11, the backstepping control generates a significant amount of torque command at the beginning of the transient to bring the motor's position up to the desired trajectory and keeps the tracking error negligible during the whole transition. In the contrary, the conventional nested PI control cannot produce enough torque command to quickly reduce the initial tracking error as shown in Figure 10.

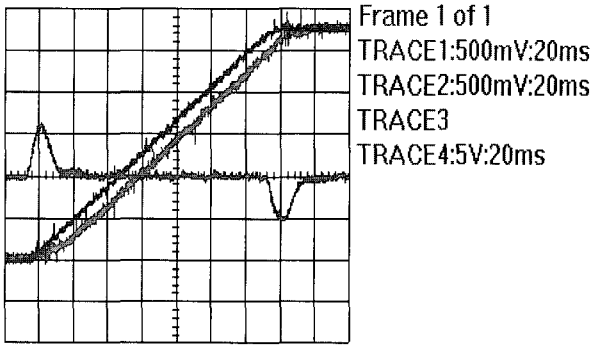


Trace 1: actual position. Trace 2: command position. Trace 4: torque command. Time: 20ms/div.

Fig. 9 Tracking performance of the nested PI controller: experimental result.

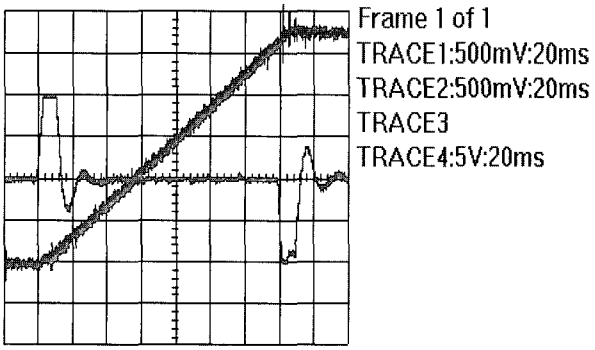


Trace 1: actual position. Trace 2: command position. Trace 4: torque command. Time: 20ms/div.

Fig. 10 Tracking performance of the integral backstepping: experiment result.

In addition, the load disturbance estimation in the control scheme given in Figure 3 is implemented in the

DSP control system and a preliminary experimental test is conducted. During the test, a continuous sinusoidal reference input signal, with period $T = 10s$, is given to the control system. The load disturbance that is estimated by the DSP is converted to an analog signal through a D/A channel. A step load disturbance is applied to the servo system at $t = 10s$, and removed at $t = 35s$. The estimated torque signal is shown in Trace 2 of Figure 11, while the corresponding actual torque command of the servo, which is issued to generate additional torque against the disturbance, is illustrated in Trace 3. The load disturbance estimator scheme is able to quickly detect the injected load disturbance. This makes it possible to use an adaptive control action to improve the robustness of the positioning control against the disturbance. A later assessment indicates a 15% increase of the position control bandwidth can be achieved by the proposed backstepping control system in accordance with the conventional control approach.

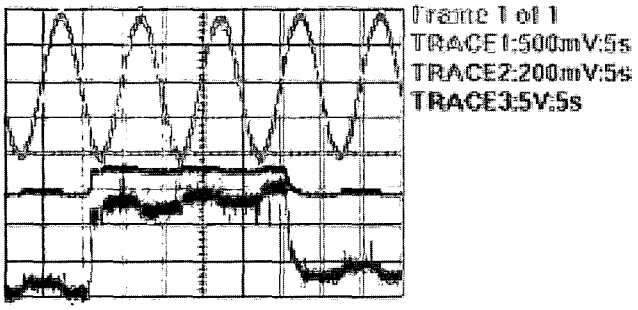


Trace 1: actual position. Trace 2: load disturbance estimate. Trace 3: torque command. Time: 5s/div.

Fig. 11 Performance test of load disturbance estimation and adaptation.

## 7. Conclusions

A practical nonlinear positioning control system based on a backstepping control approach with an integral function has been developed and presented. A systematic analysis and syntheses of the new control system has been detailed. An extension to a nonlinear adaptive control from a baseline scheme has also been discussed. This new approach improves the system's position tracking performances in terms of the response speed and bandwidth, thus benefiting industrial motion control applications. In comparison with the conventional nested PI control in a multiple-loop structure, the new scheme has a similar level of complexity and can be conveniently implemented. The final control scheme is convenient to be implemented in a practical 32-bit DSP controller, TMS320C32. The new control system can achieve superior performance over the conventional nested PI controllers, which is demonstrated by digital simulation and verified by experimental results.

## Nomenclatures

c1: gain in the position loop
c2: gain in the velocity loop
e1: position error, e1 = θref - θ
e2: velocity error, e2 = ωref - ω
J: Mechanical moment inertia
$\hat{J}$: inertia estimate
$\tilde{J}$: inertia estimation error, $\tilde{J} = J - \hat{J}$
V: Lyapunov function
Tq: motor drive acting torque command
TL: load torque
F: friction coefficient
θ: angular position of the system
θref: reference angular position
ω angular velocity
ωref: reference angular velocity
χ integral of position error
Γ: $= \frac{T_L}{J}$, weighted load disturbance
$\tilde{\Gamma} = \Gamma - \hat{\Gamma}$: error of estimated load disturbance
$\lambda_1$ : ain of the integral control at position control stage
γ1 and γ2: positive design constants of estimation.

## Acknowledgment

The authors would like to thank Chris Roche and Rockwell Automation for their valuable input and support.

Appendix A: System's asymptotic convergence

The global uniform boundedness of the position

tracking error $e_1$, the integral error signal $\chi_1$, and the velocity error signal $e_2$ are guaranteed by our selection of the Lyapunov function in (11) and non-positivity of the Lyapunov derivative in (12). Since the desired position reference signal $\theta_{ref}$ and the tracking error $e_1 = \theta_{ref} - \theta$ are bounded variables in a practical system, the actual position signal $\theta$ is globally and uniformly bounded. It can be concluded that the "virtual" control signal given in (5) is bounded based on the bounded-ness of the signals $e_1$ and $\chi_1$. Furthermore, the bounded-ness of the control torque $T_q$ becomes obvious from our choice of the controller in (9). Therefore, all the internal signals in the closed-loop motion control system in Figure 2 are bounded variables. This means that the derivatives of the error signals $e_1$ and $e_2$ are bounded as well. In other words, $\dot{e}_1, \dot{e}_2 \in L_\infty$. Based on the expression of the Lyapunov derivative in (12), we can integrate both sides from 0 to $+\infty$ and compute an energy function $V$ as:

$$V(+\infty) - V(0) = -\min\{c_1, c_2\}\left[\int_0^{+\infty} e_1^2(\tau)d\tau + \int_0^{+\infty} e_2^2(\tau)d\tau\right] \le 0, \tag{A1}$$

which can be rewritten as:

$$0 \le \left[\int_0^{+\infty} e_1^2(\tau)d\tau + \int_0^{+\infty} e_2^2(\tau)d\tau\right] \le \frac{V(0) - V(+\infty)}{\min\{c_1, c_2\}}. \tag{A2}$$

Because of the non-positivity of the Lyapunov derivative in (12), the energy function $V$ is bounded and dissipative since all the internal signals are bounded. This implies that $e_1, e_2 \in L_2$. Combining this with the fact that $e_1, e_2 \in L_\infty$, and $\dot{e}_1, \dot{e}_2 \in L_\infty$, it can be concluded that the error signals $e_1$ and $e_2$ converge to zero asymptotically. In particular, the position tracking error $e_1$ goes to zero asymptotically. In other words, the actual position $\theta$ converges to the desired reference signal $\theta_{ref}$ asymptotically in a practical system.

## References


[1] I. Kanellakopoulos and P. T. Krein, "Integral-action nonlinear control of induction motors", Proceedings of the 12th IFAC World Congress, pp. 251–254, Sydney, Australia, July 1993.

[2] M. Krstic, I. Kanellakopoulos, and P. V. Kokotovic, Nonlinear and Adaptive Control Design , New York: Wiley Interscience, 1995.

[3] R. Marino, S. Peresada and P. Valigi, "Adaptive nonlinear control of induction motors via extended matching," In P. V. Kokotovic, Foundation of Adaptive Control, Springer, Berlin, pp. 435-454, 1991.

[4] H. Tan and J. Chang, "Adaptive position Control of induction motor systems under mechanical uncertainties," Proceedings of the IEEE 1999 International Conference on Power Electronics and Drive Systems, pp. 597–602, Hongkong, July 1999.

[5] D. G. Taylor, "Nonlinear control of electric machines: an overview," IEEE Control Systems Magazine, vol. 14, No. 6, pp. 41–51, 1994.

[6] Jie Chang (Jie Zhang) and T. H. Barton, "Robust Enhancement of DC Drives with a Smooth Optimal Sliding Mode Control", IEEE Transactions on Industry Applications. Vol. 27, No. 4, July/August 1991, pp.686-693.

[7] Jie Chang (Jie Zhang) and T. H. Barton, "Microprocessor Based Primary Current Control for Cage Induction Motor Drive", IEEE Transactions on Power Electronics. Vol. 4, No. 1, Jan. 1989, pp.73-82.

[8] B.K. Bose, "Power electronics and motion control-technology status and recent trends", Power Electronics Specialists Conference, 1992, Vol.1, pp. 3 – 10.

[9] H. Fujimoto, Y. Hori; and A. Kawamura, "Perfect tracking control based on multirate feedforward control with generalized sampling periods", IEEE Transactions on Industrial Electronics, Volume 48, Issue 3, June 2001, pp. 636 – 644.

[10] Jie Chang and J. Yu, "Novel Systematic Approach of Gain Selection for Adaptive Backstepping Motion Control", The 30th Annual Conference of the IEEE Industrial Electronics Society (IECON '04), Vol 3., Nov. 2-6, 2004, pages:2447-2452.

[11] Y. Tan, Jie Chang, and H. Tan, "Adaptive Friction Compensation for Induction Motors with Inertia and Disturbance Uncertainties", The 2000 American Control Conference, Chicago, June 2000. Vol.1, pp.615-620.

**Dr. Chang** received the Ph.D. and M.Sc. degrees in electrical engineering from the University of Calgary, Calgary, Canada, respectively. He is the Associate Director of Florida Advanced Power Research Institute and Professor at Florida State University. He was a Principal Scientist and Manager of Department of Control & Power Technology at Rockwell's Corporate Research Center (RSC). He founded the Power Conversion Laboratory and Power and Control programs at RSC. Dr. Chang has assumed key industrial positions including: Project Leader, Principal Engineer, and Senior Principal Engineer at the Reliance Electric Research Center; Senior R&D engineer at Westinghouse Electric and V. P. of Engineering at TASC Drives, USA. He is a key technical contributor to several brand name AC drive products of Reliance Electric and Westinghouse, including, SA3000, SB3000, and ACUTRAL700 made in U.S.A, from fractional to 1000 horsepower. Dr. Chang holds six U.S. patents and has published over 100 refereed technical papers in IEEE Transactions, international journals and major conferences. He has been an active IEEE Senior Member since 1992. His research interests include advanced power converters, high-frequency and high-power AC motor drives, power electronics systems, renewable energy systems, real-time nonlinear and adaptive control, advanced thermal management and packaging of power devices, modeling, simulation and diagnostics of electrical machine systems.

**Yaolong Tan** received the B.S. degree from Xi'an Jiaotong University in 1993, the M.S. degree from Chinese Academy of Sciences in 1996, and the Ph.D. degree from University of California, Los Angeles, in 2000, all in electrical engineering. He worked for Rockwell Science Center at Thousand Oaks from 1999 to 2000 as a Member of Technical Staff. He worked for Voyan Technology as senior system engineer from 2000 to 2003 and for ElectriPHY Incorporation as chief architect from 2003 to 2005. He is currently serving as President and Chief Technology Officer of Triductor Technology in Silicon Valley. His major research interests include automatic control, industry automation, digital signal processing, system identification, and communication system design.